Proceedings of the 2018 IEEE
International Conference on Robotics and Biomimetics
December 12-15, 2018, Kuala Lumpur, Malaysia

A Mechanism of Single Actuator Snakeboard Robot and its Curving Motion Generation

Satoshi Ito
Faculty of Engineering
Gifu University
Gifu, Japan
email *satoshi@gifu-u.ac.jp*

Shoya Sugiura
Graduate school of Natural Science and Technology
Gifu University
Gifu, Japan
email *x4525046@edu.gifu-u.ac.jp*

Yuya Masuda
Faculty of Engineering
Gifu University
Gifu, Japan
email *s3031093@edu.gifu-u.ac.jp*

Sam Kiely
Griffith School of Engineering
Griffith University
Queensland, Australia
email *sam.kiely@griffithuni.edu.au*

Jun Yabuki
Graduate school of Engineering
Gifu University
Gifu, Japan
email *s3128024@edu.gifu-u.ac.jp*

Ryosuke Morita
Faculty of Engineering
Gifu University
Gifu, Japan
email *rmorita@gifu-u.ac.jp*

***Abstract*—This paper reports a new mechanism of a wheeled robot moving by the single actuator. This mechanism is inspired by the two-wheeled skateboard, or snakeboard. There, the control inputs are usually considered as the following three: the steering angles of the front and the rear wheels, and the torque for the rotor rotation. To propel a snakeboard with the smaller number of actuators, two steering orientations of the wheels are coupled each other at first so as to rotate in the same amount to the opposite direction synchronously. Next, the rotation of the steering orientations are connected to the rotor via the torque limiter. In addition, the stoppers are introduced to restrict and to maintain the steering orientation of the wheels. Curving the path of the robot with this mechanism to the side, the position-based control of the rotor with a drifting sine wave reference is newly proposed. The behaviors according to the control law as well as the effect of this mechanism are confirmed by a robot we construct. Consequently, some curving motion with different curvature are demonstrated. Finally, a principle of the curving motion is discussed based on the theoretical and experimental insights.**

***Index Terms*—mobile robot, snakeboard, single actuator, curving motion, torque limiter**

I. INTRODUCTION

The mobility of robots enlarges their workspace. One method to provide the mobility with the robots is to newly add some actuators. However, it is not always feasible from the aspect of the robot structure, the packaging and the cost. An alternative manner can be to place a robot on a kind of car with passive wheels and then propel the car by means of the degrees of freedom of motion of the robot itself on it: It will not require additional motors.

Such a progression is observed in the human maneuvering using a two-wheel skateboard or a snakeboad. To restrict the moving direction, the boarder adjusts the orientation of the passive wheels by giving the torsion to the board, and then twists the upper body, which produces the yaw moment to the board resulting in the driving force. The propulsion mechanism of two-wheel skateboard was investigated in detail in [1]. We also constructed its mathematical model and confirmed by the numerical simulations that sinusoidal yaw moment as well as the sinusoidal deviation of the wheel's orientations can propel the board [2]. However, we did not establish a method to control the moving direction, i.e., to make the turn or curve motion of the board.

The snakeboard was discussed in many studies from the control point of view [3]–[6]. In particular, a study by S. Iannitti *et al.* [7] kinematically calculated the deviation of the snakeboard motion in relation to the sway angle of the head and applied it to its path planning. Actually, a part of a control method proposed in this paper is the same as [7]. However, our control method didn't work well in the real robot control. Thus, we will newly propose a control law using the drifting sine wave in this paper. In addition, another important point in this paper is that we propose a robotic mechanism that achieves the snakeboard-specific movement only by the single actuator. There, the torque limiter and wheel-steering stopper are key items of our mechanism design. We will present this mechanism with its control method, and show some experimental results by this robot.

II. MECHANICAL DESIGN

A. Modeling

Although our study started with a two-wheeled skateboard [2], the snakeboard model in the 2D space is introduced as an equivalent model for considering its propulsion principle. To focus on the propulsion, the lateral balance in the original two-wheeled skateboard is assumed to be always being kept. Namely, we do not consider the lateral balance here. In this snakeboard model, the steering direction of the front and rear wheels as well as the yaw moment the boarder produces is regarded as the control inputs. Figure 1 illustrates a mathematical model we utilize for the analysis.

B. Concept

A control law for this model will be proposed in the section III. The outline of the control is almost as follows: Adjust the steering angle of the passive wheels symmetrically in the front and in the rear, i.e., change the orientation with the same magnitude in the opposite direction to each other. Then, apply the yaw moment by rotating the rotor with keeping the wheel direction. Next, reverse the wheel direction, keep them, and apply yaw moment in the reverse direction by returning the rotor. Just repeat these processes again and again.

To Realize the snakeboard mechanism, S. Iannitti *et al.* [7] designed the robot by three motors: two of them change the

978-1-7281-0376-1/18/$31.00 ©

steering angle of the front and rear wheels respectively, and the rest one drives a rotor to gain the yaw moment. We attempt to reduce the number of motors here. To do that, it will require some mechanical devices. If the change of the steering angle is restricted to be symmetrical, two coupled gears with the same number of the teeth can realize it by rotating them in anti-phase. Rather a big problem is how to drive the wheel steering and the rotor simultaneously.

From the analysis in the section III-A, we will find that the magnitude of the steering angle alternations does not have to be variable to move in the two dimensional space. This finding allows us to mechanically control the steering angle of the wheels by means of the stoppers restricting its movable range.

However, the stoppers will limit the rotor rotation at the same time if we connect them directly: this problem will be solved by disconnecting the transmission of the force to the steering rotation while the stoppers are working. The torque limiter is introduced to play this important role between the rotor and the steering mechanism. It consists of two parts and serves as a safety clutch. Normally these two parts are mechanically connected. However, when large torque is exerted, the slippage occurs on their connecting surface. This is why large torque is not transmitted through the torque limiter.

C. Mechanism

We thought up a mechanism to realize our idea in the previous section. Figure 2 illustrates our concept.

As shown in Fig. 2 (a), the upper part of the torque limiter is connected to motors, while the lower part is connected to the steering mechanism containing gear A, B and C.

When the gear A rotates, it drives the gear B and then the gear C. If the gear B and gear C have the same radius with the same number of the teeth, the amount of deviation are equal in the opposite direction. Namely, their rotations become symmetrical. Fixing the front and rear wheels to the gear B and gear C, respectively, the steering angles of two wheels can be controlled symmetrically by means of the one DoF of motion, i.e., the gear A rotation.

The sole motor on the robot rotates not only this torque limiter but also the rotor simultaneously. The rotor rotation produces the reaction force that propels the board. Thus, the rotor motion should not be restricted for the purpose of the propelling force generation. However, in our control method that will be mentioned in the section III, the steering angle must be kept constant during the period determined by the control law. Namely, the maintenance of the wheel direction limits the angle of the sole motor: That also affects the important rotor function since the motor drives both the rotor and the steering angles.

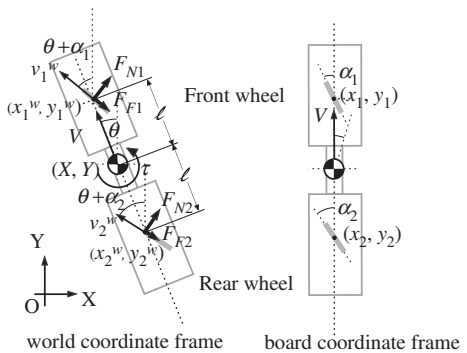

Fig. 1. Snakeboard model.

This problem will be solved by the combination of the torque limiter and the stoppers. As shown in Fig. 2 (a), the stoppers are set up to restrict the rotation of the lower part. A bar attached on the lower part prevents the lower part from rotating beyond these stoppers.

As depicted in Fig. 2(b), the steering mechanism rotates with the rotor as long as the bar does not contact to the stopper. It implies that the torque limiter is not working and the driving force is transmitted to the steering mechanism.

Then, consider the case where the bar contact to the stopper, as shown in Fig. 2 (c). The stopper stops the rotation of the lower part of the torque limiter. At this moment, the torque limiter starts working: its upper part is able to rotate even if the lower parts stop rotating. Therefore, the rotor is able to produce the propelling force against the board even if the wheel directions are maintained. Note here that the stoppers' position mechanically determines the magnitude of the steering angle to be maintained.

D. Design

We designed the snakeboard robot to realize our concept in the previous section. Figure 3 shows an overview of the robot on the left, and the stopper mechanism on the right.

To reduce the robot height, the rotor axis is separated from the axis of the wheel steering mechanism: they are connected by the same-size gears at the upper part. The robot has 270mm in height, 600mm in length and 3.8kg in weight. Its photo is shown in Fig. 4. The side supports with the omni-directional wheels prevent the robot from turning over to the lateral direction.

III. Curving control by a drifting-sine-wave rotor motion

A. Dynamics and velocity constraints

To discuss a control of the robot, the model in Fig. 1 is considered throughout this section. The motion equations with non-holonomic velocity constraint is presented in Appendix A-I. In particular, from the relation (21) and (23), the following equations hold

$$\dot{X} = -V\sin\theta \tag{1}$$

$$\dot{Y} = V\cos\theta \tag{2}$$

$$\dot{\theta} = V\frac{\tan\alpha}{\ell} \tag{3}$$

where $(X,\ Y)$ denotes the CoM position of the board, θ is board orientation from the Y axis, V denotes the speed of the robot, and ℓ is the distance from the CoM to the wheel position.

For this wheeled robot, we first propose the switching time control of steering direction. Then, we arrange it to apply to the one-actuator robot.

B. Switching time control of steering angle

In a control law we propose here, the wheel direction α is switched between α_d and $-\alpha_d$ every determined duration under the constant robot velocity V_d.

$$\alpha = \begin{cases} \alpha_d & (0 < t \le T_a(=T_1)) \\ -\alpha_d & (T_1 < t \le T_1 + T_b(=T_2)) \\ -\alpha_d & (T_2 < t \le T_2 + T_b(=T_3)) \\ \alpha_d & (T_3 < t \le T_3 + T_a(=T_4)) \end{cases} \tag{4}$$

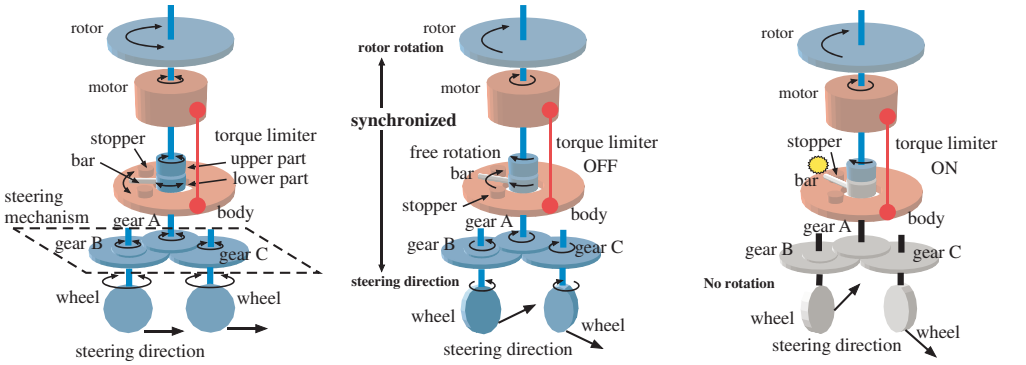

(a) Neutral (Limiter OFF) (b) Torque limiter OFF (connected) (c) Torque limiter ON (disconnected)

Fig. 2. Movement of the proposed mechanism.

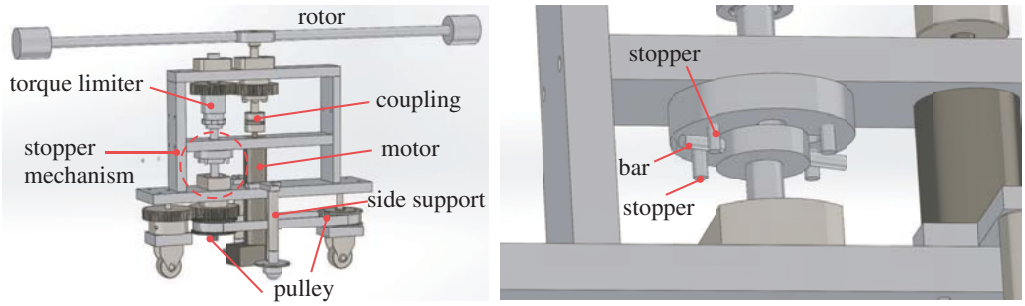

Fig. 3. A snakeboad robot with one motor.

Fig. 4. The manufactured robot.

A series of those switches is regarded as one set of control inputs. Thus, the single control period is $T_4 = 2T_a + 2T_b$. Starting from $(X, Y) = (0, 0)$ and $\theta = 0$, the position and direction of the board after one period T_4 is given as follows:

$$X(T_4) = -R_c(1 - \cos\omega_c T_4) \quad (5)$$

$$Y(T_4) = R_c \sin\omega_c T_4 \quad (6)$$

$$\theta(T_4) = \omega_c T_4 \quad (7)$$

where

$$R_c = \frac{\ell}{\tan\alpha_d}\left(\frac{2\sin\omega_d T_b}{\sin\omega_d(T_a - T_b)} + 1\right) \quad (8)$$

$$\omega_c = \omega_d \frac{(T_a - T_b)}{(T_a + T_b)} \quad (9)$$

$$\omega_d = V_d \frac{\tan\alpha_d}{\ell} \quad (10)$$

The deviation of these equations is described in Appendix A-II.

When we select T_a and T_b so as to satisfy $T_a > T_b$, R_c given by (8) becomes positive. This indicates that the center of the circle orbit comes to the left hand side, and that the board turns to the left with the radius R_c. The right turn will happen in the same way if we select as $T_a < T_b$.

When we set as $T_a = T_b$, the skateboard goes straight with undulating. The traveling distance are given as

$$Y(T_4) = \frac{4\ell}{\tan\alpha_d}\sin\frac{\omega}{4}T_4 \quad (11)$$

C. Position control to drifting sine wave reference

1) An idea: The switching time control in the above section needs the constant board velocity achieved by e.g., a method in section A-III. However, in some pilot experiments, the velocity had fluctuated because the velocity control was indirect based on the counter force of the rotor with a large inertia and thus low response. This is why we explored another method that will be easily applicable.

Although our later experiments implied that our hypothesis below did not seem correct, we initially considered that the key factor to the curving motion existed in producing the difference in the duration between the steering direction $+\alpha_d$ and $-\alpha_d$. Actually, the constant velocity is important to calculate the exact position. In our opinion, however, the velocity will be allowed to fluctuate if the purpose is only the achievement of the curved motions. Based on this idea, we aimed at adopting a manageable and popular signal, a sine wave, to achieve the curved motion.

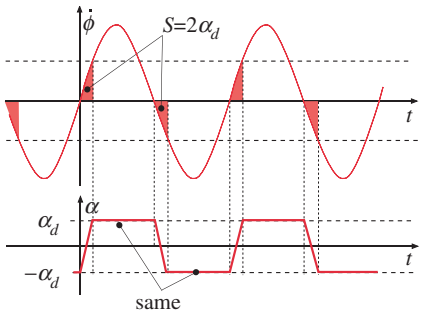

(a) without offset

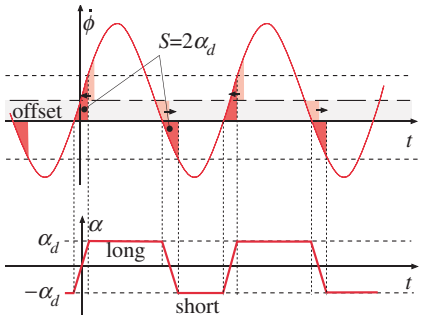

(b) with offset

Fig. 5. Change of duration in each wheel direction with respect to offset of sine-wave velocity profile.

Consider the sine wave velocity profile for the rotor, as shown in the top of Fig. 5 (a). As the rotor and the wheel direction are mechanically connected in the ratio 1:1, the complete switch to the angle $\pm\alpha_d$ requires more than or equal to $2\alpha_d$ deviations for the rotor movement. This amount is illustrated by the symmetrical regions surrounded by the sine wave and the horizontal axis. In the period outside of these regions, the stopper restricts the steering direction, though the rotor is able to rotate alone owing to the torque limiter. Therefore, the steering direction α is supposed to change as depicted at the bottom of the Fig. 5 (a): In this case, the duration of each steering direction are exactly the same.

Now, let us add the positive offset to this sine wave velocity profile, as shown in the top of the Fig. 5 (b). As the oscillation center is not zero, the regions with the area $2\alpha_d$ becomes asymmetrical. In addition, the increasing zero-crossing moves to the left, while the decreasing zero-crossing moves to the right. This produces the difference in the duration for the steering angle $+\alpha_d$ and $-\alpha_d$ as shown in the bottom of the Fig. 5 (b). We expected this difference to produce the curved motion of the robot.

2) Implementation: Because we can detect only the angle of the rotor rotation, we introduce the position control of the rotor angle. Then, the sine wave velocity profile with some offset is integrated to obtain its desired position.

$$\phi_d = A \sin 2\pi f t + \rho t \tag{12}$$

Here, ϕ_d is the desired rotor angle, A and f respectively determine the amplitude and the frequency of integrated sine wave velocity profile with some offset, the drifting sine wave, and ρ is a parameter for the drifting speed which is expected to change the curvature of the traveling orbit of the robot. The PD control is adopted for the position control:

$$\tau = -K_d\dot{\phi} + K_p(\phi_d - \phi) \tag{13}$$

where ϕ is the rotor angle detected by the rotary encoder installed in the servo-motor. K_d and K_p are the feedback gains.

IV. Experiments and Results

The object of this experiment is to confirm the generation of the curved motion by the control law (12) and (13). Our prediction is that robot goes straight at $\rho = 0$ and turn largely with larger ρ.

The robot made in the section II is controlled by the position control against the desired trajectory given as the drifting sine wave in the previous section. The controller output the torque every 1ms after the torque computation.

To obtain the position of the robot, a motion capture system is introduced. The robot is initially placed at the origin of the coordinate frame defined to the workspace to face to the positive direction of the x axis. From this same state, the robot is driven by the control law (12) and (13) in the different ρ values from 0 deg to 100 deg with 10 deg intervals. Parameters are set as $K_d = 0$, $K_p = 1$, $A = 50$ deg, $f = 0.8$ Hz. α_d is mechanically determined as 40 deg. The duration of all the experiment is 10 s.

Three experiments are conducted for each ρ value. The intermediate orbit of three is depicted for each ρ in Fig. 6.

Other experiments confirmed that the negative ρ curves the robot in the opposite direction to the positive ρ.

The last experiments attempted to bring the robot to the goal position by the feedback of the relative direction angle to the goal, namely, ρ is updated on-line by the relative direction angle. The robot adjusted the magnitude of its curved motion and finally reached the goal position, as shown in Fig. 7.

V. Discussion and Concluding Remarks

As we expected, $\rho = 0$ produced the straight line and the larger ρ curved the orbit to the left more. Rather, however, the robot tends to go straight at ρ smaller than 40 deg/s. One of the reasons might be that the velocity of the robot is far from being constant although we assumed some fluctuation: According to the observation of the robot movements, the robot obtains the reaction force from the rotor only in the short time before the rotor changes the rotational direction: the chance of the acceleration seems to be restricted to this moment. In other words, the velocity control is hard to achieve. It means that, even if the steering direction is maintained for a long time, it never prolong the moving distance to the steered direction which would have been possible under the constant velocity. This will be a reason why the robot goes straight at the small ρ.

On the contrary, the robot curves for large ρ. This is the same as we expected, but the principle of the curving motion appears to be different from our expectation. We predicted the time course of the steering direction in Fig. 8 when the robot is curving with large ρ. Then, the steering direction does not reach $-\alpha_d$, although it reaches $+\alpha$ in the opposite direction. Such an unbalance in the steering angle will cause the curving motion.

If the above consideration is true, we will be able to estimate the critical value between two mode, Fig. 5 and Fig. 8. Note here that the coupling ratio of the rotor and the steering angle is $1:1$. If there are no drifts, the steering angle given by (12) will vary in $2A$ during the half period $1/(2f)$. If the drift exists, its effect reaches $\rho/(2f)$ in the same half period

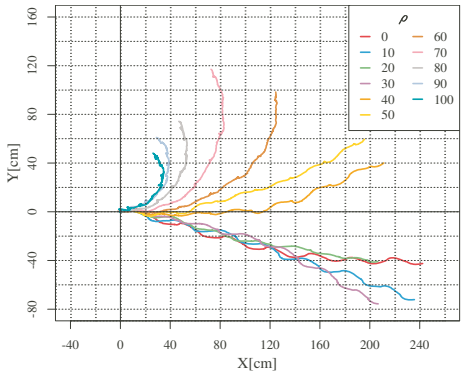

Fig. 6. Curving motion for different ρ values.

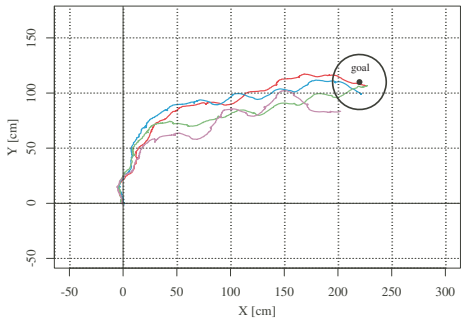

Fig. 7. Control to the goal position.

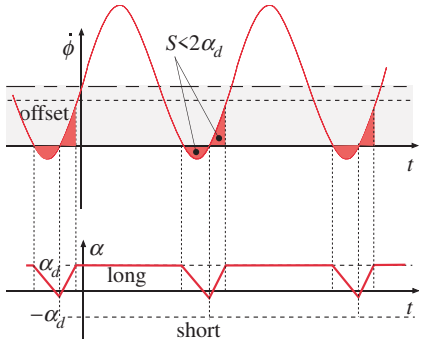

Fig. 8. Change of duration in each wheel direction with respect to a large offset of sine-wave velocity profile.

$1/(2f)$. Thus, the complete switching of the steering direction requires the relation $2A - \rho/(2f) \geq 2\alpha_d$. In summary, if ρ satisfies

$$\rho \leq 4(A - \alpha_d)f (= \rho_e) \tag{14}$$

the steering angle completely varies from α_d to $-\alpha_d$.

In the case of the experiments in Fig. 6, we can estimate $\rho_e = 32$ deg/s from $A = 50$ deg, $\alpha_d = 40$ deg, $f = 0.8$ Hz. We can observe that, for $\rho > \rho_e$, the robot curves as the mode in Fig. 8; For $\rho < \rho_e$, the robot does not curve so much. The consistence between calculation and experiment may imply the correctness of our consideration, but we have not checked the actual deviation of the steering angle yet because no sensors are installed for it. We should confirm it in our future work by building in an angle sensor such as rotary-encoder to the robot.

APPENDIX

A-I. Motion Equation with Velocity Constraints

The mechanical structure of the board in Fig. 1 is assumed symmetrical to the front-rear direction. In addition, it is assumed that the steering angles satisfy the relation $\alpha_1 = -\alpha_2 = \alpha$ as is the same as the robot we designed. Then, the motion equation becomes

$$\boldsymbol{M}\ddot{\boldsymbol{Q}} = \boldsymbol{A}_N^{\mathrm{T}}\boldsymbol{F}_N + \boldsymbol{A}_F^{\mathrm{T}}\boldsymbol{F}_F + \boldsymbol{T} \tag{15}$$

Here, $\boldsymbol{M}$ is a inertia matrix given by

$$\boldsymbol{M} = \begin{bmatrix} M & 0 & 0 \\ 0 & M & 0 \\ 0 & 0 & I \end{bmatrix} \tag{16}$$

where M is a mass of the skateboard and I is an inertial moment of the skateboard around the center of mass. $\boldsymbol{Q}$, $\boldsymbol{F}_N$, $\boldsymbol{F}_F$, $\boldsymbol{T}$ are vectors defined by

$$\boldsymbol{Q} = \begin{bmatrix} X & Y & \theta \end{bmatrix}^T \tag{17}$$

$$\boldsymbol{F}_N = \begin{bmatrix} F_{N1} & F_{N2} \end{bmatrix}^T \tag{18}$$

$$\boldsymbol{F}_F = \begin{bmatrix} F_{F1} & F_{F2} \end{bmatrix}^T \tag{19}$$

$$\boldsymbol{T} = \begin{bmatrix} 0 & 0 & \tau \end{bmatrix}^T \tag{20}$$

where, F_{Ni} is constraint force in the wheel-axis direction, F_{Fi} is viscous friction force in the steering direction, and i (=1 or 2) specifies the front or rear wheel. $\boldsymbol{A}_F$, $\boldsymbol{A}_N$ are Jacobian matrices that relate the velocity of the board state $\dot{\boldsymbol{Q}}$ with each component of the wheels' velocities $(\dot{x}_i^w, \dot{y}_i^w)$. These matrices are defined later in (25) and (22), respectively.

It is assumed that two wheels do not slip in the wheel axis direction. This assumption is expressed as the velocity constraints:

$$\boldsymbol{A}_N\dot{\boldsymbol{Q}} = \boldsymbol{0} \tag{21}$$

$$\boldsymbol{A}_N = \begin{bmatrix} \cos(\theta+\alpha) & \sin(\theta+\alpha) & -\ell\cos\alpha \\ \cos(\theta-\alpha) & \sin(\theta-\alpha) & \ell\cos\alpha \end{bmatrix} \tag{22}$$

As for the wheel velocity v_i^w, the following relation holds.

$$-\boldsymbol{A}_F\dot{\boldsymbol{Q}} = \boldsymbol{V}^w \tag{23}$$

where

$$\boldsymbol{V}^w = \begin{bmatrix} v_1^w & v_2^w \end{bmatrix} \tag{24}$$

$$\boldsymbol{A}_F = \begin{bmatrix} \sin(\theta+\alpha) & -\cos(\theta+\alpha) & -\ell\sin\alpha \\ \sin(\theta-\alpha) & -\cos(\theta-\alpha) & \ell\sin\alpha \end{bmatrix} \tag{25}$$

Assuming the viscous friction is given as

$$F_i^F = B_i v_i^w \tag{26}$$

we finally obtain the following dynamics

$$\boldsymbol{M}\ddot{\boldsymbol{Q}} - \boldsymbol{A}_N^{\mathrm{T}}\boldsymbol{F}_N = -\boldsymbol{A}_F^{\mathrm{T}}\boldsymbol{B}\boldsymbol{A}_F\dot{\boldsymbol{Q}} + \boldsymbol{T} \tag{27}$$

where $\boldsymbol{B} = \mathrm{diag}[B_1, B_2]$ is the viscous coefficient at each wheel. With the time derivative of (21), the motion equation of the board with velocity constrains become

$$\begin{bmatrix} \boldsymbol{M} & -\boldsymbol{A}_N^{\mathrm{T}} \\ -\boldsymbol{A}_N & 0 \end{bmatrix} \begin{bmatrix} \ddot{\boldsymbol{Q}} \\ \boldsymbol{F}_N \end{bmatrix} = \begin{bmatrix} -\boldsymbol{A}_F^{\mathrm{T}}\boldsymbol{B}\boldsymbol{A}_F \\ \dot{\boldsymbol{A}}_N \end{bmatrix} \dot{\boldsymbol{Q}} + \begin{bmatrix} \boldsymbol{T} \\ \boldsymbol{0} \end{bmatrix} \tag{28}$$

A-II. Motion by switching time control of the steering angle

When the speed of the robot V and the steering angle α are kept to the constant desired value V_d and α_d respectively, the right hand side of (3) becomes constant value, ω_d. Then, we can integrate (3) easily, which gives the following equation:

$$\theta(t) = \omega_d t \tag{29}$$

Integrating (1), (2) and (3) from $t = 0$ to $t = T$ with the initial condition $X(0) = Y(0) = \theta(0) = 0$, we obtain

$$X(T) = -\frac{\ell}{\tan\alpha_d}\{1 - \cos\omega_d T\} \tag{30}$$

$$Y(T) = \frac{\ell}{\tan\alpha_d}\sin\omega_d T \tag{31}$$

$$\theta(T) = V_d\frac{\tan\alpha_d}{\ell}T = \omega_d T \tag{32}$$

Based on these results, the position of the board at T_1, T_2, T_3 and T_4 are given as:

$$X(T_1) = \frac{\ell}{\tan\alpha_d}\cos\omega T_a \tag{33}$$

$$Y(T_1) = \frac{\ell}{\tan\alpha_d}\sin\omega T_a \tag{34}$$

$$\begin{aligned} X(T_3) &= X(T_1) + \frac{\ell}{\tan\alpha_d}\{(1-\cos 2\omega T_b)\cos\omega T_a \\ &\quad - \sin 2\omega T_b \sin\omega T_a\} \\ Y(T_3) &= Y(T_1) + \frac{\ell}{\tan\alpha_d}\{(1-\cos 2\omega T_b)\sin\omega T_a \\ &\quad + \sin 2\omega T_b \cos\omega T_a\} \end{aligned} \tag{35}$$

$$\begin{aligned} X(T_4) &= X(T_3) \\ &\quad + \frac{\ell}{\tan\alpha_d}\{-(1-\cos\omega T_a)\cos\omega(T_a - 2T_b) \\ &\quad - \sin\omega T_a \sin\omega(T_a - 2T_b)\} \end{aligned} \tag{36}$$

$$\begin{aligned} Y(T_4) &= Y(T_3) \\ &\quad + \frac{\ell}{\tan\alpha_d}\{-(1-\cos\omega T_a)\sin\omega(T_a - 2T_b) \\ &\quad + \sin\omega T_a \cos\omega(T_a - 2T_b)\} \end{aligned} \tag{37}$$

After some calculations, we finally obtain (5), (6) and (7). If a series of inputs (4) is repeated n times, the board potion and orientation becomes

$$X(nT_4) = -R_c(1 - \cos n\omega_c T_4) \tag{38}$$

$$Y(nT_4) = R_c \sin n\omega_c T_4 \tag{39}$$

$$\theta(nT_4) = n\omega_c T_4 \tag{40}$$

Eliminating T_4 using (38) and (39), the equation of the circle orbit are obtained

$$(X(nT_4) + R_c)^2 + Y(nT_4)^2 = R_c^2 \tag{41}$$

whose center is located at $(-R_c, 0)$ and whose radius is $|R_c|$.

A-III. Velocity control

In order to apply (30), (31) and (32), its velocity has to be keep to V_d. For this velocity control, we utilize the torque τ.

The V is expressed as follows using (3):

$$V = \frac{\ell}{\tan\alpha_d}\dot{\theta} \tag{42}$$

Its time-derivative is

$$\dot{V} = \frac{\ell}{\tan\alpha_d}\ddot{\theta} \tag{43}$$

On the other hand, from (28), $\ddot{\theta}$ can be written with τ as follows:

$$\ddot{\theta} = N(\boldsymbol{Q}, \dot{\boldsymbol{Q}}) + M(\boldsymbol{Q})\tau \tag{44}$$

Here, N and M are the scalar functions of $\boldsymbol{Q}$ and $\dot{\boldsymbol{Q}}$. Substituting (43) with (44), we have

$$\dot{V} = \frac{\ell}{\tan\alpha_d}(N(\boldsymbol{Q}, \dot{\boldsymbol{Q}}) + M(\boldsymbol{Q})\tau) \tag{45}$$

The right hand side of the above equation should be $K(V_d - V)$, because the time evolution of V becomes

$$\dot{V} = K(V_d - V) \tag{46}$$

and thus

$$V(t) = V_d - V(0)\exp(-Kt) + \to V_d \tag{47}$$

Here, K is a positive constant corresponding to the control gain. Therefore, the following equation must be satisfied:

$$\frac{\ell}{\tan\alpha_d}(N(\boldsymbol{Q}, \dot{\boldsymbol{Q}}) + M(\boldsymbol{Q})\tau) = K(V_d - V) \tag{48}$$

Solving it to τ, we finally obtain the control law:

$$\tau = \frac{\tan\alpha_d}{\ell}\cdot\frac{K(V_d - V)}{M} - \frac{N}{M} \tag{49}$$

This ensures that V converges to and is maintained to V_d .

References

[1] T. Wang, B. Su, S. Kuang, and J. Wang, "On kinematic mechanism of a two-wheel skateboard: The essboard," *Journal of Mechanisms and Robotics*, vol. 5, no. 3, p. 034503, 2013.

[2] S. Ito, S. Takeuchi, and M. Sasaki, "Motion measurement of a two-wheeled skateboard and its dynamical simulation," *Applied Mathematical Modelling*, vol. 36, no. 5, pp. 2178–2191, 2012.

[3] J. Ostrowski, "Steering for a class of dynamic nonholonomic systems," *IEEE Transactions on Automatic Control*, vol. 45, no. 8, pp. 1492–1498, 2000.

[4] E. Shammas, H. Choset, and A. Rizzi, "Towards automated gait generation for dynamic systems with non-holonomic constraints," in *Proceedings 2006 IEEE International Conference on Robotics and Automation*, 2006, pp. 1630–1636.

[5] T. Narikiyo, "Control of underactuated mechanical systems via passive velocity field control: Application to snakeboard and 3D rigid body," *Nonlinear Analysis*, vol. 71, pp. e2358–e2365, 2009.

[6] E. Shammas and M. De Oliveira, "Motion planning for the snakeboard," *The International Journal of Robotics Research*, vol. 31, no. 7, pp. 872–885, 2012.

[7] S. Iannitti and K. Lynch, "Minimum control-switch motions for the snakeboard: A case study in kinematically controllable underactuated systems," *IEEE Transactions on Robotics*, vol. 20, no. 6, pp. 994–1006, 2004.